Hydrodynamics and Kinetics of Phenols Removal from Industrial Wastewater in a Trickle Bed Reactor (Part I: Hydrodynamic Study)

doi: 10.15255/CABEQ.2013.1772

M. F. Abid,* F. T. Jasim, and L. S. Ahmed
Chemical Engineering Department, University of Technology, P.O.35010, Baghdad, Iraq

Original scientific paper
Received: February 8, 2013
Accepted: August 30, 2014

An experimental investigation of the hydrodynamic parameters in a trickle bed reactor is presented. The operating conditions are selected for the operating system to be at trickle flow regime. The effects of the two-phase flow rates, reactor pressure and temperature on the pressure drop, external liquid holdup and liquid axial dispersion are discussed. Pressure drop was measured using differential pressure transducer, while liquid holdup and axial dispersion were estimated using RTD technique with a reactive dye as a tracer. The results confirmed that pressure drop is proportional to flow rate of fluids and operating pressure while it is inversely proportional to temperature. Liquid flow rate has a proportional effect on liquid holdup and axial dispersion while gas flow rate and temperature presented a different image. A comparison between the results of present work and that of literature is presented and discussed. Empirical correlations for pressure drop, liquid holdup and axial dispersion with operating conditions are developed with correlation coefficient of 98.4 to 99.7 %.

Key words:
trickle bed reactor, pressure drop, liquid holdup, liquid axial dispersion, RTD

Introduction

Industrial processes use significant amounts of water which require treatment before discharging to surface water system.[1] Aqueous wastes having an organic pollutant load in the range of few hundred to few thousand ppms are too dilute to incinerate but yet too toxic. Phenol is one of the most common organic water pollutants present in wastewater of various industries such as refineries (6–500 mg L^{-1}), coking operations (23–3900 mg L^{-1}), coal processing (9–6800 mg L^{-1}), manufacture of petrochemical (28–1220 mg L^{-1}), and also in pharmaceutical, plastics, wood products, paint and pulp and paper industries (0.1–1600 mg L^{-1}).[2] At present, several treatment methods are available: chemical, physical (adsorption, reverse osmosis), biological, wet air oxidation (CWO), and incineration. In selecting a wastewater treatment process among these methods, one should take into account the toxicities and concentration of the pollutants in the waste stream.[3] The wet-air or thermal liquid-phase oxidation (WAO) process, in which the generation of active oxygen species, such as hydroxyl radicals, takes place at high temperatures and pressures, is known to have a great potential for the treatment of effluents containing a high content of organic matter, or toxic contaminants for which direct biological purification is unfeasible. In this process, molecular oxygen dissolved in the wastewater reacts with the organic and inorganic pollutants. The oxidizing power of the process is based on the high solubility of oxygen at these severe conditions and the high temperature that increases the reaction rates and production of free radicals.[4] To reduce the cost, catalyst is added to lower the reaction temperature and pressure, which is referred to as CWAO process. The catalyst is usually made of transitional metal salt/metal oxide. By using CWAO, the oxidation of phenol can be tremendously facilitated at milder conditions as low temperature.[5] The selection of a suitable reactor is one of the key criterion that affects the industrial implementation of advanced wastewater treatment facilities. The large experience on the operation of TBRs in industrial hydro-treatment processes makes them the first choice for the performance of CWAO reactions.[6] Trickle-bed reactors are the most widely used type of three-phase reactors. They are employed in petroleum, petrochemical and chemical industries, in waste treatment and in biochemical and electrochemical processing as well as other application.[7] Gas and liquid concurrently flow downward over a fixed bed of catalyst particles. The liquid phase flows over the catalyst as a thin film, while the gas phase flows continuously between the catalysts.[8–10] Various flow regimes exist in TBRs depending on the superficial mass velocity, fluid properties and bed characteristics are (trickle flow, pulsing

*Corresponding author: email: dr_mfa@uotechnology.edu.iq, mobile: +9647709229217

flow, mist flow and bubble flow).[11,12] The hydrodynamic parameters (i.e., flow regime, gas and liquid superficial velocities, gas and liquid holdups, and axial dispersion coefficient) are key parameters for design, scale-up, and control of trickle-bed reactors. The present work aims to study the hydrodynamics and kinetics characterestics of a trickle bed reactor for phenol degradation in wastewater by investigating the applicability of a commercial 0.5 % platinum/alumina catalyst, which is used currently for desulfurization process in North Refinery Company-Iraq. Also it is to investigate the effects of studied operating conditions (LHSV, superficial gas velocity, temperature, reactor pressure and initial phenol concentration) on the hydrodynamic and kinetic parameters of the operating system (phenol and oxygen).

Materials and methods

Experimental setup and procedure

A schematic illustration of the experimental facility setup is shown in Fig. 1. Experimental reactor was made up of stainless steel tube able to withstand temperature up to 140 ºC and pressures up to 4 MPa with 0.05 m inside diameter and 5 mm wall thickness packed with (800 g and 0.6 m height) of catalyst particles. Table 1 represents some characteristics of catalyst, pre and post packing, trickle bed reactor and material used through the experiment. The trickle bed reactor was packed with different packing layers of inert particles besides the catalyst layer. Firstly, 0.2 m from the top a layer (pre-packing) of 2 mm × 2 mm glass cylinder was set just before the catalyst bed in order to ensure uniform radial liquid distribution over the reactor cross-section, then 0.5 % Pt/Al_2O_3 catalyst particles bed with a height of 0.6 m. The last layer (post-packing) again contains 2 mm × 2 mm glass cylinder particles with a height of 0.45 m, which supports the catalyst packing to complete a total bed height of 1.25 m. The reactor to particle diameter ratio of 31.25 was sufficient to prevent wall effect.[13] The packing was maintained by means of a stainless steel screen placed at the column bottom and had a mesh openings large enough to prevent art factual bed flooding but narrow enough to impede particle crossings. This configuration is used in kinetic and hydrodynamic experiments. To measure the two-phase pressure drop through the reactor bed, pressure taps were drilled in the reactor head and in the bottom of the reactor and a differential pressure transducer was mounted. The output signal of the transducer was fed to an A/D converter and stored in PC, with sampling frequency of 250 Hz. The reactor was externally heated with electrical tape heater (Heraeus-Wittmann GmbH Heidelberg, type MS6) which was connected to a temperature controller (Yang Ming CX TA 3000) that maintained the bed temperature within ±3 °C of the set point temperature by means of an on-off regulator control which manipulated the heat supply of the external tap heater. After the synthetic solution was heated with an immersed electric heater in the storage tank of 100-L capacity up to a maximum of 60 °C it was pumped by means of a metering pump (Dose pump, BALDOR FRUM DUTY, USA) to a high-pressure small stainless steel tank of 0.04 id and 0.35 m length to damp the pulsation due to pumping. The gas was delivered from a high-pressure cylinder equipped with a pressure regulator to adjust the operating pressure. A flow meter coupled with needle valve enabled the gas flow rate to be set and measured. The liquid and gas streams were mixed and preheated in the pre-heater before entering the reactor at the top through a distributor containing 29 holes (φ = 0.5 mm). Discharged fluids (gas and liquid) from the reactor flow through the gas-liquid separator. In the top flange of the separator, stainless steel mesh demister was placed to trap the liquid mist from the effluent gas stream. Pressure indicator and safety valve was mounted to prevent pressure build up in the gas and liquid delivery and exit streams. A one-way valve was located in gas and liquid line to assure the flow in one direction. A 1.5 L-steel vessel filled with known amount of dye solution, was connected to the top of TBR via an on-off solenoid valve which energized with time relay. The system included three valves; two of them were used for filling the vessel with tracer and pumping air while the third was being used for injecting the tracer into the reactor through a pulse-type input response. Table 1 presents the specification of reactor, catalyst, bed, and operating parameters used in the present study. The characteristics of phenol and dye used are presented in Table 2. Table 3 shows the variation of density and viscosity of water and air with temperature.

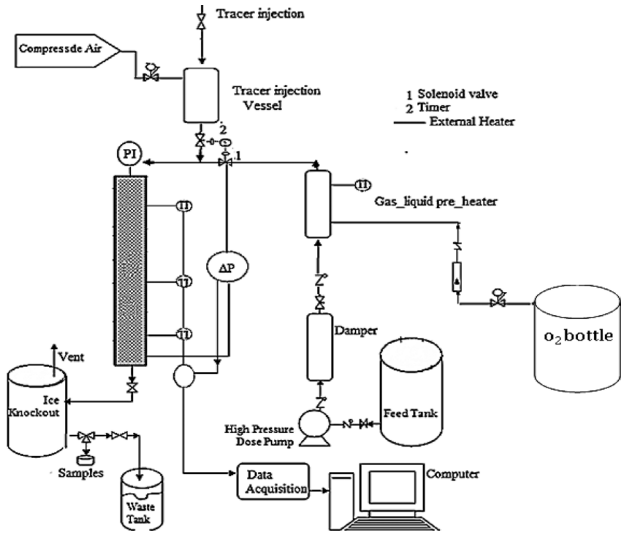

Fig. 1 – *Schematic diagram for the experimental setup*

Table 1 – *Characteristics of reactor, bed, catalyst and operating conditions*

Reactor properties		Catalyst properties	
Reactor diameter (i.d.)	0.05 m	Active metal	0.5 % Pt
Total length	1.25 m	Catalyst carrier	γ-Al_2O_3
Type of inert bed	Glass beads 3x3 mm	Particle shape	Sphere
Prepacking depth	0.15 m	Specific surface area	250 $m^2\,g^{-1}$
Pellet porosity	0.52	Pellet density	0.56 g cm^{-3}
Bed porosity	0.38–0.4		
Catalyst bed depth	0.6 m		
Operating conditions			
Bed temperature		25–140 °C	
Reactor pressure		0.1–0.6 MPa	
Superficial gas velocity		0.018–0.25 m s^{-1}	
Superficial liquid velocity		0.0013–0.1 m s^{-1}	

Table 2 – *Characteristics of phenol and dye used in the present work*

Phenol characteristics	
Color	White
pH	(4.5–6)
Molecular weight, g mol^{-1}	94.11
Chemical formula	C_6H_6O
Purity	99.5 %
Freezing point, ºC	(40–41)
Dye characteristics	
Type of dye	Reactive red
Commercial name	Forosyn red
Chemical formula	$C_{26}H_{21}N_5Na_4O_{19}S_6$
Molecular weight, g mol^{-1}	991.82
Wave length (λ), nm	485

Table 3 – *Variation of density and viscosity of water and air with temperature*

Temperature (°C)	Water[20]		Air[21]	
	viscosity, μPa s	density, kg m^{-3}	viscosity, μPa s	density, kg m^{-3}
20	1002	998.23	18.20	1.205
30	797.2	995.67		
40	653.5	992.25	19.13	1.127
50	547.1	988.07		
60	466.6	983.24	20.16	1.067
70	400.9	977.81		

Hydrodynamics experiments

Hydrodynamic experiments were aimed to study the effect of operating conditions such as reactor pressure, bed temperature, superficial gas and liquid velocity on the hydrodynamic parameter (i.e., pressure drop, liquid holdup and axial dispersion).

Pressure drop

Before starting, the reactor is operated in high interaction regime at high liquid flow rate for at least 30 min after the bed is heated up to 10 °C above the desired temperature, followed by reducing the liquid flow rate to the desired level. This helps to achieve perfect bed pre-wetting and prevents hysteresis effects.[14] This procedure was repeated for each experiment. The data for pressure drop measurements were collected for a period of at least 10 minutes with sampling frequency of 250 Hz.

Liquid holdup and axial dispersion

The dynamic liquid holdup and axial dispersion were determined by using tracer technique method. Before starting the experiment, the bed was fully wetted by passing water at a slightly higher rate. Then the flow rates of air and water were adjusted to the desired values. It took approximately 30 minutes to attain steady state. The attainment of steady state was determined by measuring the flow rates of gas and liquid at the outlet. It was observed that the flow rates did not change after 30 minutes of operation. The pulse of tracer was then injected through the pneumatic injection system connected with an on–off solenoid valve opened with time relay 5 seconds and then closed. Samples were drawn from the bottom of reactor in each run to evaluate the change of tracer concentration with time every 4 seconds. RTD curve was constructed and a statistical method (i.e., slope method) and used to estimate axial dispersion coefficient.[15]

Analytical procedures

To measure tracer (i.e., dye) concentration in the reactor effluent, JASCO ultraviolet/visible (UV-VIS/530) spectrophotometer was used. Prior to measuring, a dye calibration curve was constructed by collecting samples of stocks solution in the range of (0.5–1991 mg L^{-1}) and measuring their light absorbency against each concentration then plotting concentration values against light absorbency. Fig. 2 illustrates the calibration curve.

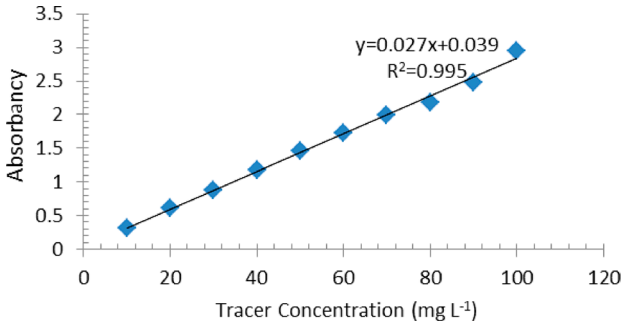

Fig. 2 – *Calibration curve of reactive red dye*

Theoretical aspects

The liquid holdup and dispersion coefficient were calculated using the tracer RTD data from experiments.

Liquid holdup[16]

$$\varepsilon_L = \frac{t_m \Phi_L}{V_R} \tag{1}$$

where t_m, Φ_L and V_R are mean residence time (s), volumetric flow rate of liquid ($m^3\ s^{-1}$) and reactor volume (m^3), respectively.

$$t_m = \frac{\int_0^\infty t C_i \mathrm{d}t}{\int_0^\infty C_i \mathrm{d}t} \cong \frac{\Sigma t C_i \Delta t}{\Sigma C_i \Delta t} \tag{2}$$

Axial dispersion coefficient[17] DaxL

$$D_{axl} = \frac{U_L \sigma_\theta^2 L}{2} \tag{3}$$

where,

$$\sigma_\theta^2 = \left(\frac{U_L}{L}\right)^2 \sigma^2 \tag{4}$$

$$\sigma_i^2 = \frac{\int_0^\infty t^2 C_i \mathrm{d}t}{\int_0^\infty C_i \mathrm{d}t} - (t_m)^2 \cong \frac{\Sigma t^2 C_i \Delta t}{\Sigma C_i \Delta t} - (t_m)^2 \tag{5}$$

Results and discussion

Pressure drop

In the present work, the pressure drop through the bed was measured by using pressure transducer, recording the pressure fluctuations (signals). Fig. 3 shows samples of pressure drop oscillation versus time. The pressure drop increased proportionally with reactor pressure, superficial gas and liquid velocity while decreasing with temperature. To determine the pressure drop of various signals from recorded sets of data over a period of time, the average value is calculated.

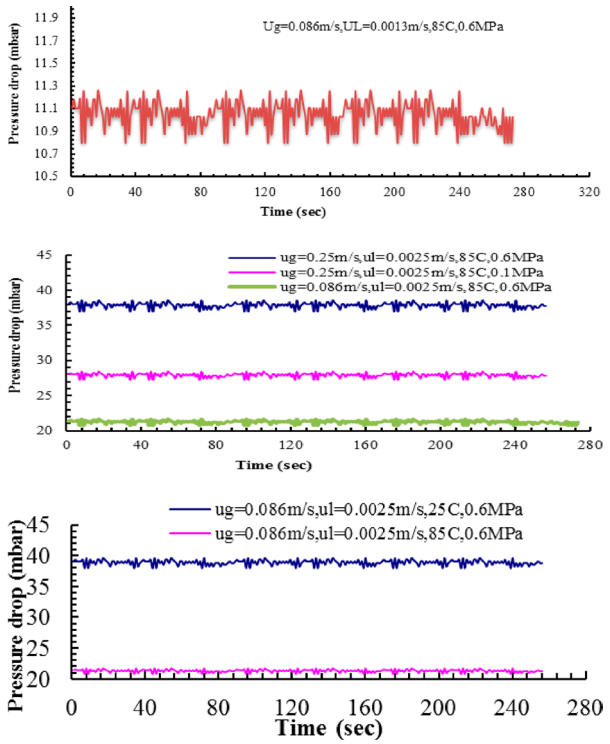

Fig. 3 – *Pressure drop signals at different operating conditions*

Liquid holdup and axial dispersion

The tracer technique, was used to measure the liquid holdup and axial dispersion. Liquid holdup and dispersion coefficient could be evaluated by recording the shape of the tracer curve as it passed the exit of the reactor. In particular, the mean time of passage (from eq. 2) and the spread of the curve (from eq. 5) were measured. Fig. 4 depicts a comparison between exper-

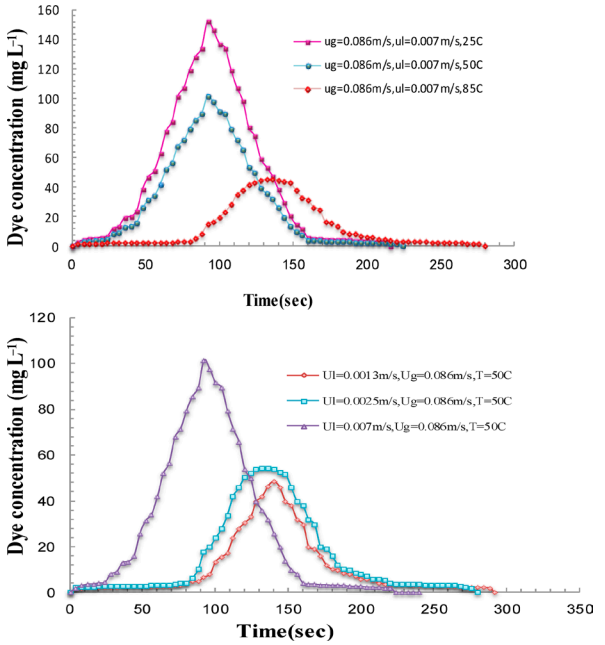

Fig. 4 – *RTD curves of tracer output response at different operating conditions*

imental RTD curves at different sets of temperature, superficial gas and liquid velocities. Some notes can be concluded from Fig. 4, the mean residence time of the RTD curve decreased, as the liquid flow rate increased. Also, as the liquid velocity increased, the RTD curve increasingly deviated from symmetry which means that more back mixing occurred in the liquid phase. The mean residence time of the RTD curve increased with increasing of reactor temperature leading to lower back mixing. The peak of each curve represents the maximum concentration of tracer at the effluent of reactor at specified time which depends on the operating conditions applied.

Effect of operating conditions on hydrodynamic parameters

Operating pressure

Fig. 5 depicts the effect of superficial gas and liquid velocities on pressure drop. As expected, the Figure shows a proportional relationship between pressure drop and superficial gas and liquid velocities at studied conditions. The increasing pressure drop may be attributed to the increased shear stresses exerted by the drag forces between the phases. As can be seen the pressure drop is more sensitive to velocity changes than to pressure changes. This result is attributed to the fact that with pressure changes, elevated pressure results in higher gas density, which consequently produces a higher drag force at the gas-liquid interface and lower inertia force of the gas-phase. However with velocity changes, at high superficial gas velocity, the pressure drop increases in comparison to the gravitational force which is more affected than the drag force at high pressure and low gas velocity. Our results are in agreement with that of.[18,14,19] Fig. 5 illustrates the effect of operating temperature on the pressure gradient along the reactor for various superficial gas and liquid velocities and pressure. Also the pressure drop decreased with increasing temperature. As indicated before, under the present conditions, pressure drop strongly affected by viscosity, density, surface tension and velocity of the fluids. As the liquid viscosity decreases with respect to temperature, the gas viscosity follows a different trend the net of shear stress at the gas-liquid and liquid-solid interfaces is not obvious. Table 3 shows the variation of density and viscosity of water and air with temperature. As can be seen from Table 3 the effect of temperature on liquid viscosity is more pronounced in comparison to that on gas viscosity. The frictional forces at the gas-liquid and liquid-solid interfaces are decreased with increased temperature.

An additional contributing factor in favor of influence is that the pressure drop decreases with elevated temperatures due to the decrease in gas phase inertia with temperature (via gas density). Also at high superficial gas and liquid velocities, the effect of temperature on pressure drop is more significant. These results are in agreement with findings of.[22–24] Fig. 5 also shows the comparison between the present work and that of.[12]

Liquid holdup

Liquid holdup results from the balance between the driving forces and the resistances. Fig. 6 shows a proportional trend between superficial liquid velocity and liquid holdup at a given superficial gas velocity, while superficial gas velocity gives an opposite effect on the liquid holdup. The increase in liquid holdup with liquid throughput is due to film thickening on the catalyst particle. The reduction in liquid holdup with gas flow is attributed to the drag force at the gas-liquid interface, which is a driving force for the co-current liquid flow. This drag force depends on gas velocity and density. Hence, the drag force increases with gas velocity and density, shorter liquid

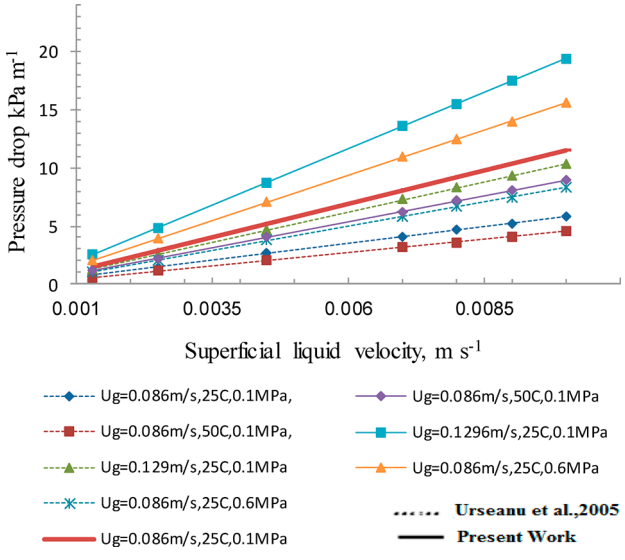

Fig. 5 – *Effect of operating parameters on pressure drop*

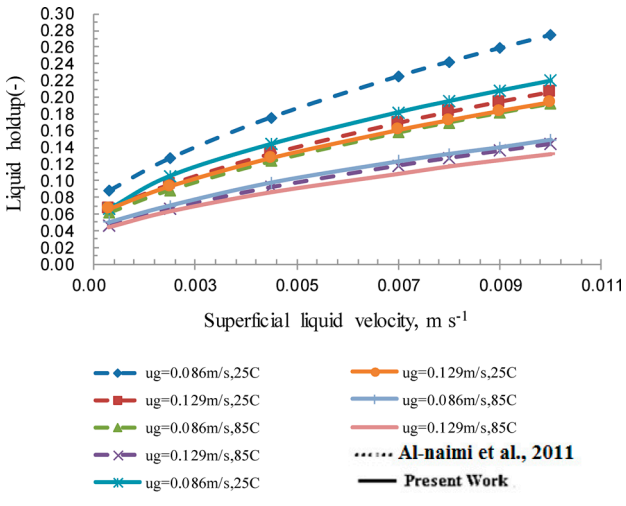

Fig. 6 – *Effect of operating parameters on liquid holdup*

mean residence time results in a reduction in liquid holdup. These results are in agreement with findings of.[25,26] As can be seen from Fig. 6, the liquid holdup is inversely proportional to the operating temperature. The liquid holdup decreases with increasing temperature at constant superficial liquid and gas velocities. This can be explained by a decrease in liquid viscosity as temperature increases, so the shear stress at the gas liquid and liquid - solid interfaces decreases resulting in lower liquid holdup. The liquid surface tension decreased with increased temperature causing a discontinuity of liquid film flow. The results of the present work are in agreement with findings of.[22,25] Fig. 6 shows the comparison between the present work with data of.[25]

Quantitatively, the mean relative deviation of the present work from that of [23] was 8.7 % to 13.2 %. This could be acceptable from experimental stastics point of view. This deviation may be attributed to the contribution of two effects, the first resulted from the applicability of eq. 2 which is usually used for constant-density system. The second source of deviation may resulted from the measurements of light absorbancy.

Liquid axial dispersion

Fig. 7 illustrates the effect of temperature, and superficial gas and liquid velocities on the liquid axial dispersion coefficient at given operating pressure. The Figure shows a positive trend between liquid velocity and dispersion coefficient while the effects of gas velocity and temperature on axial dispersion shows a different image. Larger liquid throughputs yield larger axial dispersion. This is due to increased backmixing in the liquid-phase. The negative impact of temperature on liquid viscosity is relatively high. This decrease of viscosity with increased temperature has a remarkable decrease of liquid holdup which can be presented as an explanation for the decrease in axial dispersion with temperature. Gas flow rate has also an opposite effect on axial dispersion since increased gas flow rate reduced liquid film on catalyst particles with a reduction in liquid holdup. Consequently, backmixing was reduced. These results are in fair agreement with findings of.[22,26,27] Fig. 7 also shows a comparison between the present work and the data of.[22] The values of axial dispersion found with the work of[22] are lower than our experimental data. One possible cause for the observed mismatch is the differences in the geometric variables of the experimental setups.

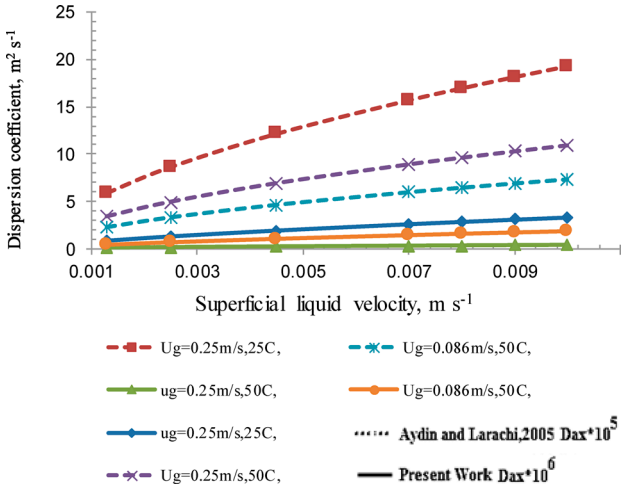

Fig. 7 – *Effect of operating parameters on liquid axial dispersion coefficient*

Empirical correlations

Pressure drop, dynamic liquid holdup and axial dispersion coefficient were correlated in this work with the operating parameters, as follows:

$$\varepsilon_L \alpha U_L,\ \frac{1}{U_g, T} \tag{6}$$

$$\Delta P \alpha U_L,\ U_g,\ P,\ \frac{1}{T} \tag{7}$$

$$D_{ax} \alpha U_L,\ \frac{1}{U_g},\ \frac{1}{T} \tag{8}$$

Therefore, the following power-law correlations are proposed to predict pressure drop, dynamic liquid holdup, and axial dispersion coefficient under the operating range of the studied operating parameters:

$$\frac{\Delta P}{\Delta z} = a_0 U_g^{b_0} U_l^{c_0} \rho_G^{d_0} \mu_L^{e_0} \tag{9}$$

$$\varepsilon_L = a_1 Re_L^{b_1} Re_g^{c_1} Ga_L^{d_1} \tag{10}$$

$$D_{ax} = a_2 Re_L^{b_2} Re_g^{c_2} Ga_L^{d_2} \tag{11}$$

The pressure drop, dynamic liquid holdup, and axial dispersion coefficient data were fitted to the form of eqs. (9, 10, and 11) by non-linear least-squares regression analysis, the exponents a_i, b_i, c_i, and d_i were estimated as presented in Table 4.

Table 4 – *Proposed correlations for the hydrodynamics parameter*

Hydrodynamics parameter	Proposed correlation	Statistics
Pressure drop	$\frac{\Delta P}{Z} = 5.6836 \cdot 10^4 U_G^{0.51} U_L^{0.88} \rho_G^{0.18} \mu_L^{0.47}$	R^2= 98.47 %
Liquid holdup	$\varepsilon_L = 3.329 \cdot 10^2 Re_L^{0.5377} Re_g^{-0.3053} Ga_L^{-0.51}$	R^2= 99.22 %
Liquid axial dispersion	$D_{ax} = 0.0000134 Re_L^{0.7} Re_g^{-0.53} Gs_L^{-0.32}$	R^2= 99.70 %

Fig. 8 plots a comparison between the experimenal and theoretical values of pressure drop, liquid holdup, and liquid axial dispersion coefficients, respectively. The agreements of the experimenal results with the theoretical outcomes of pressure drop, liquid holdup, and liquid axial dispersion coefficients were 98.47 %, 99.22 % and 99.7 % , respectively.

The comparison of the correlations of the present work with other related correlations available in the literature, which are presented in Table 5, are shown in Figs. 9, 10 and 11 for preesure drop, liquid holdup and liquid axial dispersion, respectively. It can be seen that, qualititavely, the related correlations have the same trends with operating variables. However, quantitavily some deviations ocurred between the objective response of the related correlations. These deviations may be attributed to the differences in geometric variables of the various experimental setups used. The second source of deviation may have resulted from the measurements techniques. These deviations could be acceptable from an engineering point of view. Results of axial dispersion shown in Fig. 11 indicate that the present system was more closer to ideal flow behaviour than that of[16] (Saroha *et al.*, 2006).

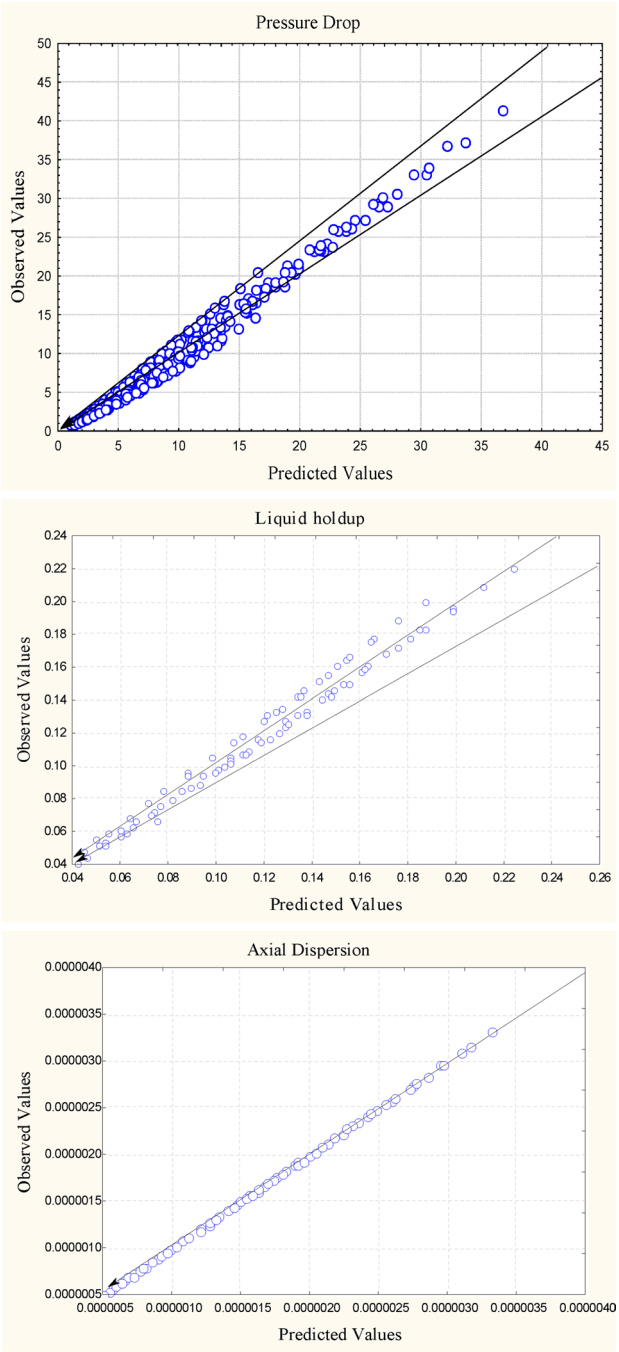

Fig. 8 – *Observed and predicted values of pressure drop (a), holdup (b) and axial dispersion (c)*

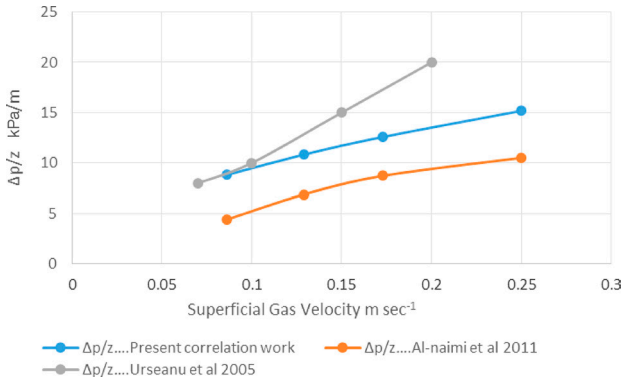

Fig. 9 – *Variation of axial pressure drop against gas velocity at 25 ˚C , 0.1 MPa and U_L = 0.008 m s^{-1}*

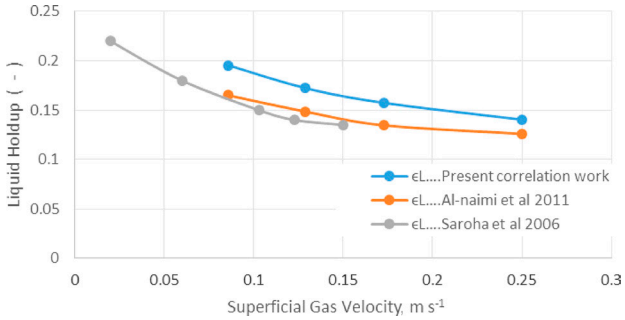

Fig. 10 – *Variation of liquid holdup against gas velocity at 25 ˚C , 0.1 MPa and U_L = 0.008 m s^{-1}*

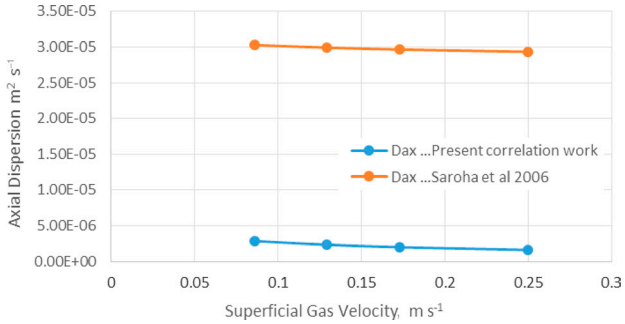

Fig. 11 – *Variation of liquid axial dispersion against gas velocity at 25 ˚C , 0.1 MPa and U_L = 0.008 m s^{-1}*

Table 5 – *Related correlations of pressure drop, liquid holdup and liquid axial dispersion used from literature*

Reference	Proposed correlation	Hydrodynamics parameter
12	$\frac{\Delta P}{Z} = 16 U_L^{0.54} \rho_G^{0.17} f_w^{0.5} d_p^{-2.76}$	Pressure drop
23	$\frac{\Delta P/Z}{\rho_L g} = 5.9869 \cdot 10^{-3} Re_L^{0.34383} Re_g^{0.13224} w_{e_L}^{0.14} G_{a_L}^{0.4464}$	
23	$\varepsilon_L = 0.13676 Re_L'^{0.27946} Re_G^{-0.03643} \left(G_{a_L} \left(1 + \frac{\Delta P/H}{\rho_L g} \right) \right)^{-0.44184} W_{e_L}^{0.25458}$	Liquid holdup
16	$Pe_L = 5.35 Re_L^{0.53} Re_g^{0.03}$	Liquid axial dispersion

Conclusion

Studies on the CWO of phenol illustrate the potential of CWO process as an efficient treatment technology for industrial wastewater. The hydrodynamic parameters (i.e., flow regime, gas and liquid superficial velocities, gas and liquid holdups, and axial dispersion coefficient) are key parameters for design, scale-up, and control of trickle-bed reactors. The following conclusions could be drawn from the present study.

1. Liquid superficial velocity has a positive impact on pressure drop, liquid holdup and liquid axial dispersion.

2. Increasing gas superficial velocity caused an increase in pressure drop and decrease in liquid holdup and axial dispersion.

3. Increasing of reactor pressure caused an increase in two-phase pressure drop

4. Pressure drop, liquid holdup, and axial dispersion were negatively affected by increased temperature.

5. Power law-based correlations developed in this present work have good reliability compared with experimental results.

6. Comparison of the developed correlations of the present work with other related correlations available in literature reveals good agreement from the engineering point of view.

ACKNOWLEDGMENTS

Authors were grateful to the chemical Engineering Department-University of Technology for providing space and facilities. Thanks were also due to Prof. Saba Ghani and MSc. Safa Mohammad of University of Tikrit for their valuable assistance.

Notations

C – Dye concentration in liquid phase, mg L^{-1}
d_p – Catalyst particle diameter, m
D_{axL} – Liquid axial dispersion coefficient, m^2 s^{-1}
G_{aL} – Modified Galilo number $\left(= \frac{\rho_L^2 d_p^2 g \varepsilon^3}{\mu_L^2 (1-\varepsilon)^3} \right)$, –
L – Tested length of reactor, m
P – Reactor pressure, MPa
ΔP – Pressure drop, kPa
R_{eg} – Gas Reynolds number $\left(\frac{u_G d_p \rho_G}{(1-\varepsilon)\mu_G} \right)$
R_{eL} – Liquid Reynolds number
t – time, s
t_m – Mean residence time, s
U_g – Superficial gas velocity, m s^{-1}
U_L – Superficial liquid velocity, m s^{-1}
V_R – Reactor volume, m^3

Greek Symbols

ε – Bed voidage, –
ε_G – Gas Holdup, –
ε_L – Dynamic liquid Holdup, –
Φ_L – Liquid volumetric flow rate, m^3 s^{-1}
μ – Viscosity, kg m^{-1} s^{-1}
ρ_b – bed density, kg m^{-3}
ρ_L – Density of liquid, kg m^{-3}
ρ_g – Density of gas, kg m^{-3}
σ – Variance, s^2
σ_θ – Variance, –

References

1. *Tansel, B.,* Chem. Eng. J. **1** (2008) 17. http://dx.doi.org/10.2174/2211334710801010017
2. *Gutierrez, M., Pina, P., Torres, M., Cauqui, M. A., Herguido, J.,* Catalysis Today **149** (2010) 326. http://dx.doi.org/10.1016/j.cattod.2009.05.027
3. *Guo, J., Al-Dahhan, M. H.,* Chem. Eng. Sci. **60** (2005) 735. http://dx.doi.org/10.1016/j.ces.2004.08.043
4. *Roy, S., Vashishtha, M., Saroha, A. K.,* J. Eng. Sci. Tech. Rev. **3**(1) (2010) 95.

5. *Wu, Q., Hu, X., Yue, P.,* Chem. Eng. Sci. **58** (2003) 923. http://dx.doi.org/10.1016/S0009–2509(02)00628–0
6. *Eftaxias, A.,* Catalytic wet air oxidation of phenol in a trickle bed reactor: kinetics and reactor modelling, PhD thesis, Rovira i Virgili University, 2002.
7. *Saroha, A. K., Nadi, I.,* Chem. Eng. Sci. **63** (2008) 3114. http://dx.doi.org/10.1016/j.ces.2008.03.023
8. *Propp, R. M., Colella, P., Crutchfield, W. Y., Day, M. S.,* J. Comp. Phy. **165** (2000) 311. http://dx.doi.org/10.1006/jcph.2000.6604
9. *Kundu, A., Saroha, A. K., Nigam, K. D. P.,* Chem. Eng. Sci. **56** (2001) 5963. DOI: 10.1016/S0009–2509(01)00250–0
10. *Lopes, R. J. G., Quinta-Ferreira, R. M.,* Ind. Chem. Eng. **49** (2010) 1105. http://dx.doi.org/10.1021/ie900767q
11. *Al-Dahhan, M. H., Dudukovic, M. P.,* Chem. Eng. Sci. **49** (1994) 5681. http://dx.doi.org/10.1016/0009–2509(94)00315–7
12. *Urseanu, M. I., Boelhouwer, J. G., Bosman, H. J. M., Schroijen, J. C., Kwant, G.,* Chem. Eng. J. **111** (2005) 5. http://dx.doi.org/10.1016/j.cej.2005.04.015
13. *Al-Dahhan, M. H., Larachi, F., Dudukovic, M. P., Laurent, A.,* Ind. Eng. Chem. Res. **36** (1997) 3292. http://dx.doi.org/10.1021/ie9700829
14. *Al-Dahhan, M. H., Dudukovic, M. P.,* Chem. Eng. Sci. **49** (1994) 5681. http://dx.doi.org/10.1016/0009–2509(94)00315–7
15. *Bashi, H. Y., Gunn, D.,* Chem. Eng. Sci. **35** (1980) 2405. http://dx.doi.org/10.1016/0009–2509(80)85053–6
16. *Saroha, A. K., Khera, R.,* Chem. Eng. and Proc. **45** (2006) 455. http://dx.doi.org/10.1016/j.cep.2005.11.005
17. *Chander, A., Kundu, A., Bej, S. K., Dalai, A. K., Vohra, D. K.,* Fuel **80** (2001) 1043. http://dx.doi.org/10.1016/S0016–2361(00)00170–8
18. *Wammes, W. J. A., Middelkamp, J., Huisman, W. J., Debeas, C. M., Westerterp, K. R.,* AIChE. J. **37** (1991) 1849. http://dx.doi.org/10.1002/aic.690371210
19. *Iluita, I., Thyrion, F. C., Muntean, O.,* Chem. Eng. Sci. **51** (1996) 4987. http://dx.doi.org/10.1016/0009–2509(96)00331–4
20. *Korson, L., Drost-Hansen, W., Millero, F. J.,* Phys. Chem. J. **75** (2016) 1969.
21. www.EngineeringToolBox.com
22. *Aydin, B., Larachi, F.,* Chem. Eng. Sci. **60** (2005) 6687. http://dx.doi.org/10.1016/j.ces.2005.05.065
23. *Aydin, B., Larachi, F*., Chem. Eng. J. **143** (2008) 236. http://dx.doi.org/10.1016/j.cej.2008.04.013
24. *Al-Naimi, S. A., Al-Sudani, F. T. J., Halabia, E. K.,* Chem. Eng. Res. Des. **89**(7) http://dx.doi.org/10.1016/j.cherd.2010.11.008
25. *Guo, J., Al-Dahhan, M. H.,* Chem. Eng. Sci. **59** (2004) 5387. http://dx.doi.org/10.1016/j.ces.2004.07.106
26. *Aydin, B.,* Hydrodynamic of trickle bed reactors: steady and non-steady state operations, PhD Thesis, university of Laval, 2008.
27. *Houwelingen, A. J. V., Merwe, W. V. D., Wales, N., Heydenrych, M., Nicol, W.,* Chem. Eng. Res. & Des. J. **87** (2009) 677. http://dx.doi.org/10.1016/j.cherd.2008.10.003